Supporting Information for

Presence and Absence of Excited State Intramolecular Charge Transfer with the Six Isomers of Dicyano-*N*,*N*-Dimethylaniline and Dicyano-(*N*-Methyl,*N*-Isopropyl)aniline

Victor A. GALIEVSKY,*[,a,b] Sergey I. DRUZHININ,[a] Attila DEMETER,[a,c] Sergey A. KOVALENKO,*[,d] Tamara SENYUSHKINA,[a] Peter MAYER,[e] Klaas A. ZACHARIASSE,*[,a]

[a]Max-Planck-Institut für biophysikalische Chemie, Spektroskopie und Photochemische Kinetik, 37070 Göttingen, Germany

[b]B.I. Stepanov Institute of Physics, National Academy of Sciences of Belarus, pr. Nezavisimosti 68, 220072 Minsk, Belarus

[c]Institute of Materials and Environmental Chemistry, Chemical Research Center, Hungarian Academy of Sciences. P.O.Box 17, 1525 Budapest, Hungary

[d]Institut für Chemie, Humboldt Universität zu Berlin, Brook-Taylor Strasse 2, 12489 Berlin, Germany

[e]Department Chemie und Biochemie, Ludwig-Maximilians-Universität, Butenandtstrasse 5-13, Haus F, 81377 München, Germany
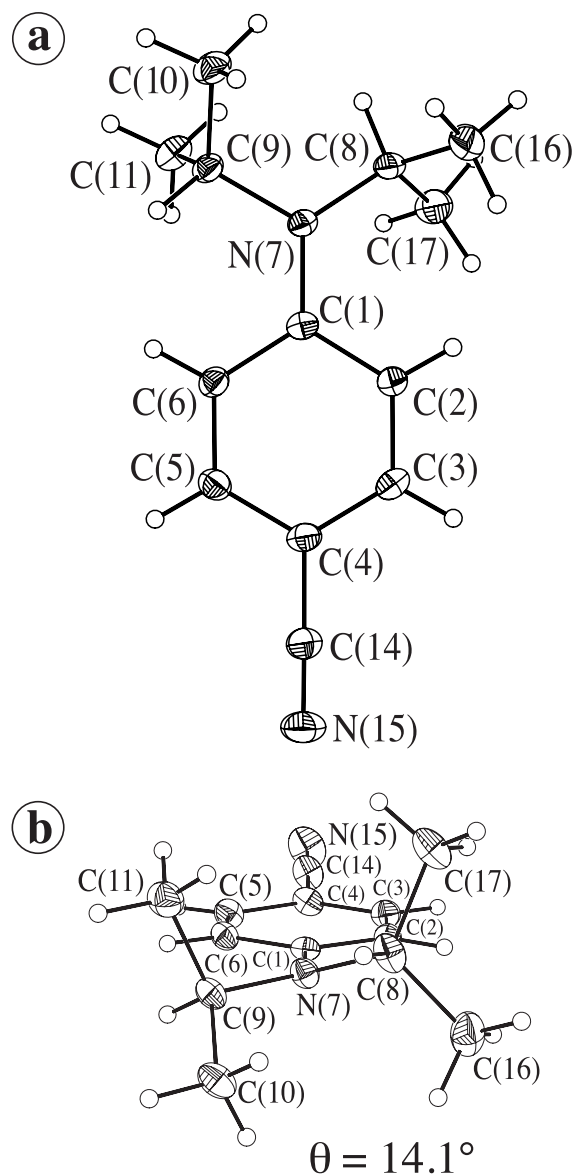
Figure S1. Crystal structures of DIABN. A view from above (a) and one along the axis from the amino group to the dicyanobenzene moiety (b) is presented. The amino twist angle θ is defined as (C(8)N(7)C(1)C(2) + C(9)N(7)C(1)C(6))/2. The pyramidal angle φ is the angle between the vector N(7)C(1) and the plane C(8)N(7)C(9). See Chart 4 and Table 1.
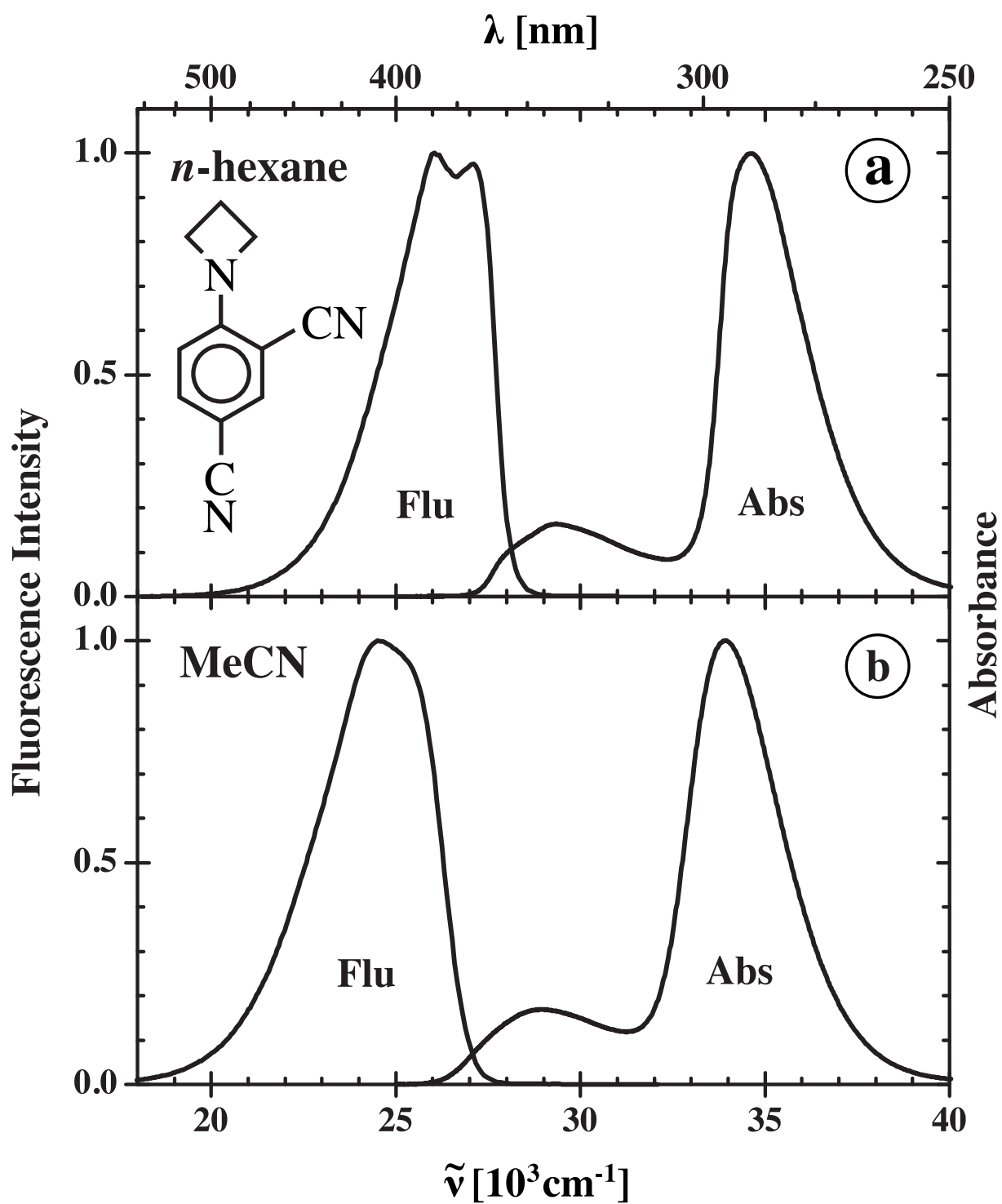
Figure S2. Fluorescence (LE) and absorption (Abs) spectra of the *N*-(2,4-dicyanophenyl)azetidine (24DCP4C) (Chart 2) in (a) *n*-hexane and (b) acetonitrile (MeCN) at 25 $^\circ$C. The fluorescence spectra are attributed to the emission from a locally excited (LE) state, see text.
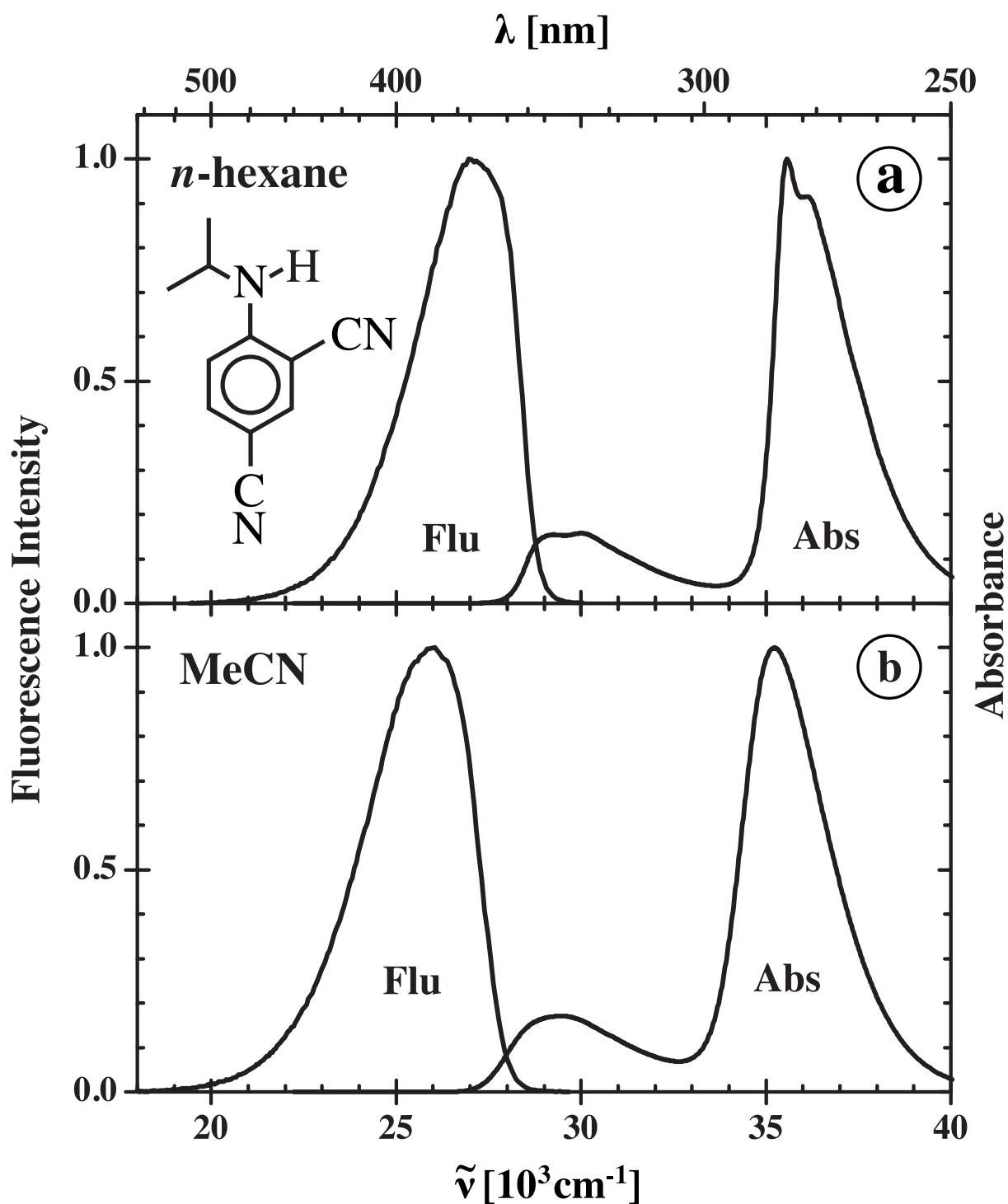
Figure S3. Fluorescence (LE) and absorption (Abs) spectra of the 2,4-dicyano-*N*-isopropylaniline (24DCIA) (Chart 3) in (a) *n*-hexane and (b) acetonitrile (MeCN) at 25 $^{\circ}$C. The fluorescence spectra are attributed to the emission from a locally excited (LE) state, see text.

TABLE S1: Oxidation Potentials E(D/D$^+$) and Vertical Ionization Energies (vIE) of Aliphatic Amines

| amine	E(D/D$^+$) V/SCE	vIE (eV)
iPrN(Me)$_2$	**0.84**[1]	8.20[2,3]
HN(Et)$_2$	**1.12**[4]	8.63[5]
HN(Pr)$_2$	**1.06**[4]	8.54[5]
HN(iPr)$_2$	**1.06**[4]	8.40[5]
N(Me)$_3$	**1.05**[6,7]	8.54[3]
MeN(Et)$_2$	**0.91**[7]	8.32[3]
1-methylpiperidine	**0.96**[4]	8.35[3]

(1) Extrapolated value, see Figure S4. (2) Nelsen, S. F. *J. Org. Chem.* **1984**, *49*, 1891. (3) Cherkasov, A. R.; Jonnsson, M.; Galkin, V. *J. Mol. Graphics Mod.* **1999**, *17*, 28. (4) X. Allonas, private communication. (5) Aue, D. H.; Webb, H. M.; Bowers, M. T. *J. Am. Chem. Soc.* **1976**, *98*, 311. (6) Mann, C. K. *Anal. Chem.* **1964**, *36*, 2424. (7) Zachariasse, K. A.; Druzhinin, S. I.; Galievsky, V. A.; Demeter, A.; Allonas, X.; Kovalenko, S. A.; Senyushkina, T. A. *J. Phys. Chem. A* **2010**, *114*, 13031.
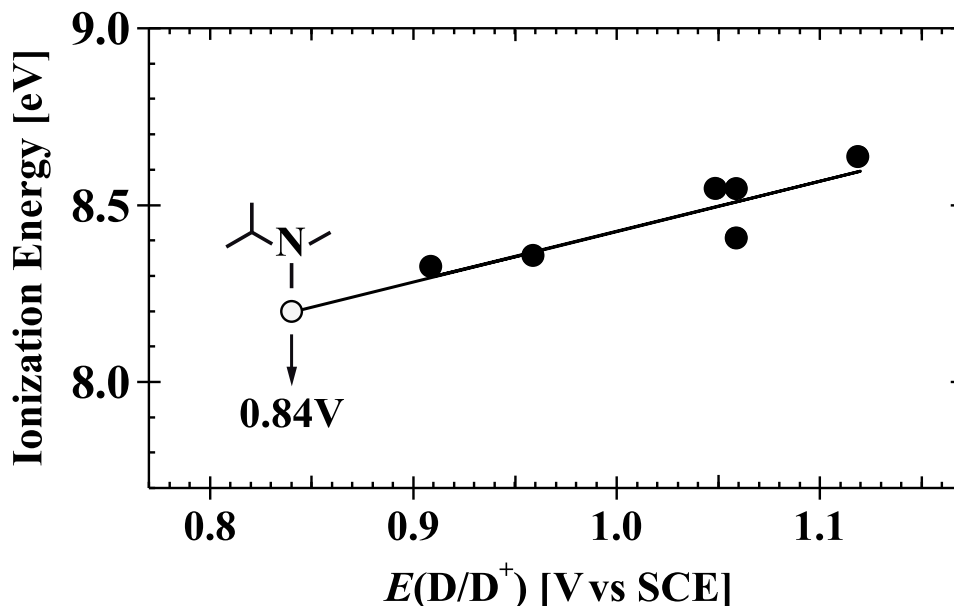
Figure S4. Plot of of vertical ionization energy vIE (eV) vs the oxidation potential E(D/D$^+$) (vs SCE) of aliphatic amines. By extrapolation, E(D/D$^+$) = 0.84 V vs SCE is determined for iPrN(Me)2 with vIE = 0.82, see Table S1.
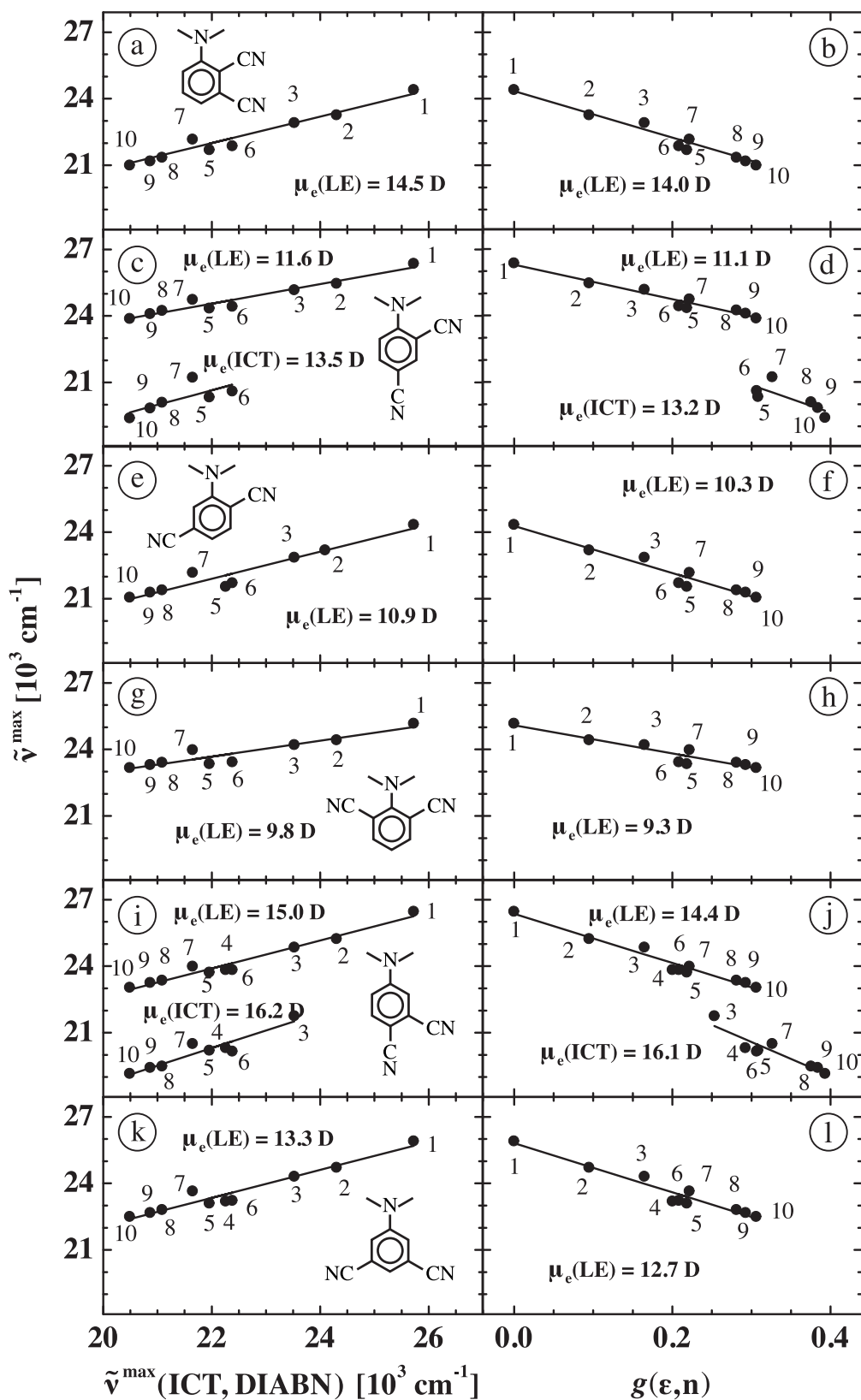
Figure S5. Solvatochromic plots of the LE and ICT fluorescence maxima $\tilde{\nu}^{\,max}$ (LE) and $\tilde{\nu}^{\,max}$ (ICT) of the six mnDCDMAs (a,c,e,g,i,k) vs $\tilde{\nu}^{\,max}$ (ICT) of DIABN (eqs 4-6) and (b,d,f,h,j,l) the solvent polarity parameter $g(\varepsilon,n)$. For LE, $g(\varepsilon,n) = f(\varepsilon) - f(n^2)$, whereas for ICT $g(\varepsilon,n) = f(\varepsilon) - \frac{1}{2}f(n^2)$, see Table 7 and text. The $\tilde{\nu}^{\,max}$ data and the numbering of the solvents are given in Table 7. From the slopes of the plots, the LE and ICT dipole moments μ_e(LE) and μ_e(ICT), indicated in the Figures, are calculated (Table 8).

6
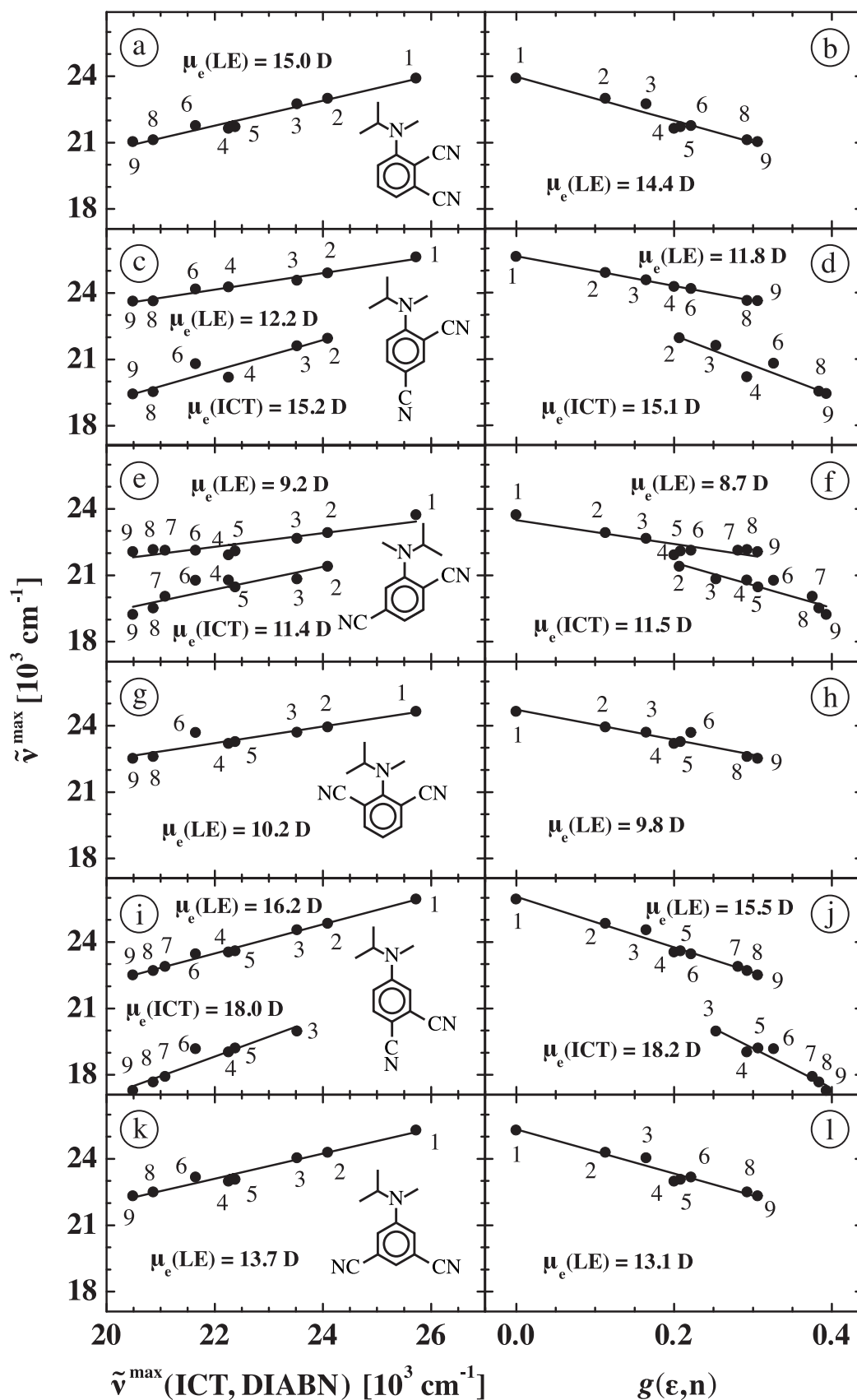
Figure S6. Solvatochromic plots of the LE and ICT fluorescence maxima $\tilde{\nu}^{max}$ (LE) and $\tilde{\nu}^{max}$ (ICT) of the six mnDCMIAs (a,c,e,g,i,k) vs $\tilde{\nu}^{max}$ (ICT) of DIABN (eqs 4-6) and (b,d,f,h,j,l) the solvent polarity parameter $g(\varepsilon,n)$. For LE, $g(\varepsilon,n) = f(\varepsilon) - f(n^2)$, whereas for ICT $g(\varepsilon,n) = f(\varepsilon) - \frac{1}{2}f(n^2)$, see Table 9 and text. The $\tilde{\nu}^{max}$ data and the numbering of the solvents are given in Table 9. From the slopes of the plots, the LE and ICT dipole moments μ_e(LE) and μ_e(ICT), indicated in the Figures, are calculated (Table 10).

7

TABLE S2: Fluorescence Decay Times and Kinetic Parameters (Eqs 7-9, Scheme 1) of the ICT Reaction of 25DCMIA in MeCN, PrCN, and THF

solvent	T [^{o}C]	ε	n	τ_2 [ps]	τ_1 [ps]	A_{12}/A_{11} (eq 9)	k_a [10^{10} s^{-1}]	k_d [10^{10} s^{-1}]	τ'_o(ICT) [ns]
MeCN	-44.0[a]	49.9	1.3743	1.4	2340	114	70.8	0.62	2.32
MeCN	-30.0	46.6	1.3677	0.7	2520	288	142	0.49	2.51
MeCN	-19.8	44.5	1.3629	0.2	2480	76	494	6.5	2.45
PrCN	-39.9[b]	34.0	1.4138	2.5	4190	48	39.2	0.82	4.13
PrCN	-50.2	36.3	1.4189	2.8	4070	70	35.2	0.50	4.03
PrCN	-60.0	38.7	1.4238	4.2	3960	74	23.5	0.32	3.92
PrCN	-70.0	41.5	1.4286	5.1	3860	74	19.3	0.26	3.82
PrCN	-80.0	44.8	1.4334	5.1	3790	116	19.4	0.17	3.77
PrCN	-90.0	48.6	1.4380	5.9	3750	108	16.8	0.16	3.72
PrCN	-100.7	53.4	1.4428	8.9	3800	121	11.1	0.092	3.78
PrCN	-110.0	58.4	1.4468	5.5	4280	212	18.1	0.085	4.27
THF	-60.2[c]	11.0	1.4529	7.4	5160	9.0	12.2	1.35	4.81
THF	-70.1	11.6	1.4585	9.4	4880	9.7	9.6	0.99	4.56
THF	-80.2	12.3	1.4642	10.0	4590	13.0	9.3	0.71	4.36
THF	-90.0	13.0	1.4696	12.2	4340	16.3	7.7	0.47	4.16
THF	-99.8	13.9	1.4748	13.9	4120	23.6	6.9	0.29	4.00
THF	-104.8	14.3	1.4774	11.0	4030	29.1	8.8	0.30	3.93
THF	-104.9	14.3	1.4775	16.6	3920	25.1	5.8	0.23	3.81
THF	-105.3	14.4	1.4777	12.0	4030	27.7	8.0	0.29	3.93

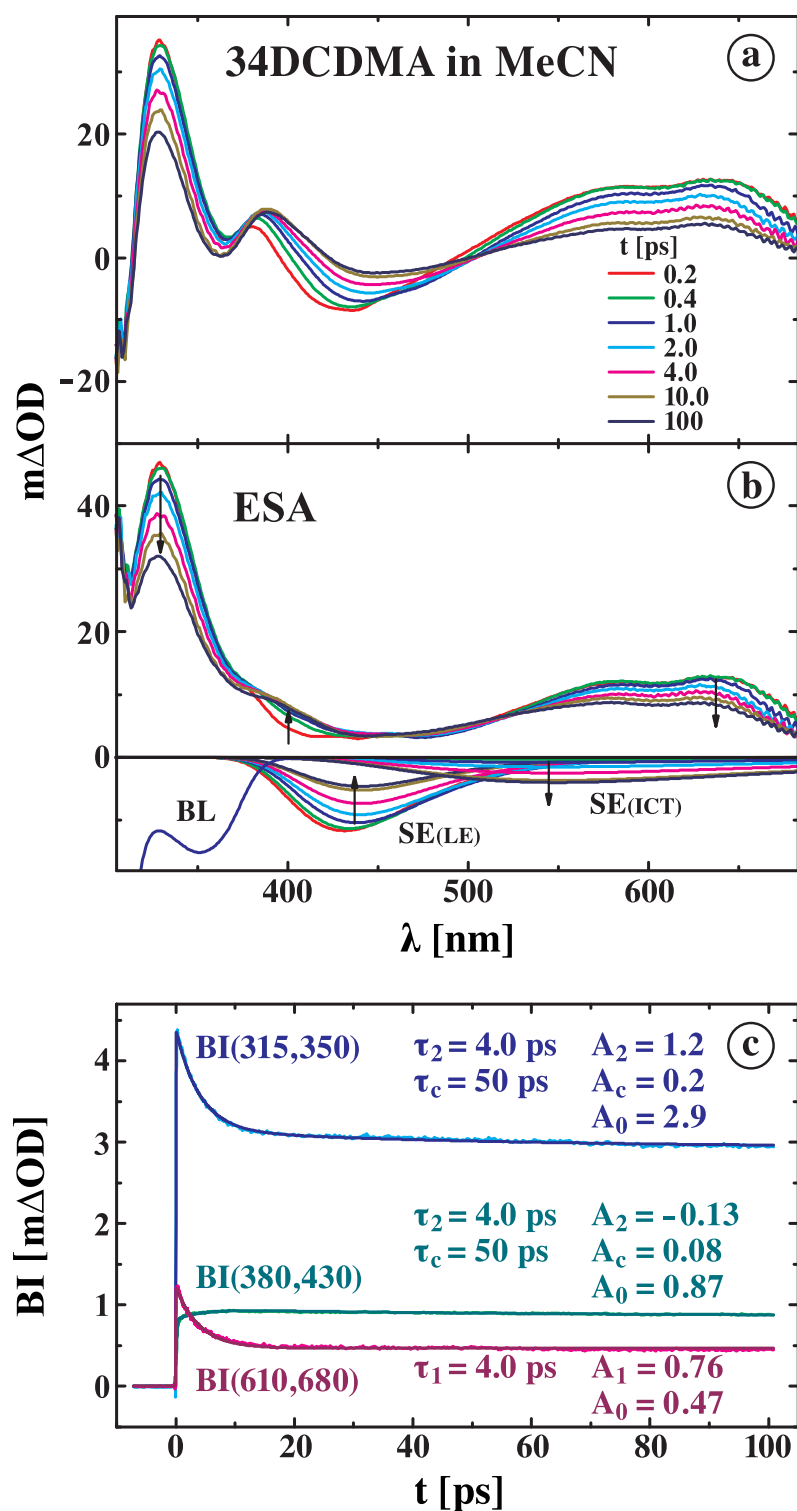[a]Figure 11a. [b]Figure 11b. [c]Figure 11c.

24DCDMA in MeCN (0.2-100 ps).
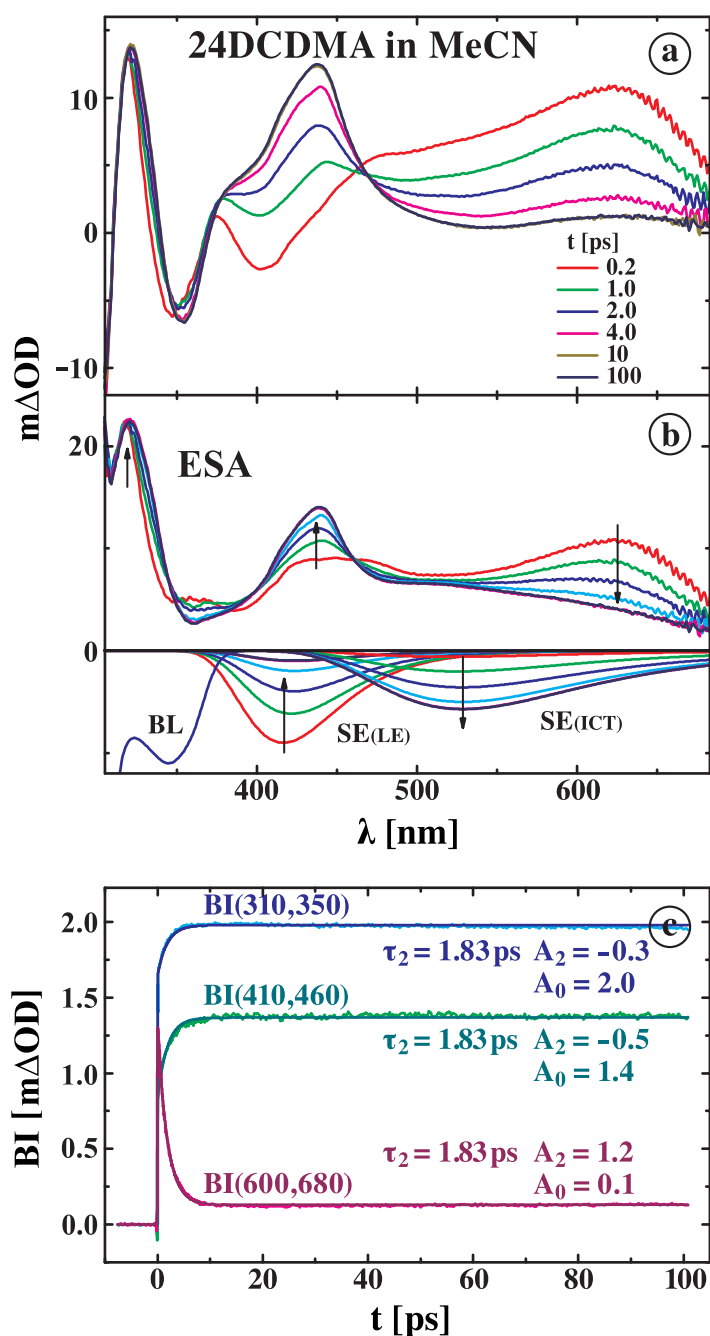
Figure S7. 24DCDMA in MeCN at 361 nm excitation (305-683 nm). (a) Transient absorption spectra and (b) excited state absorption (ESA) spectra, at pump-probe delay times between 0.2 and 100 ps, after subtraction of the bleach (BL) spectrum and stimulated emission from LE and ICT (SE(LE) and SE(ICT)). The BL and SE (for fluorescence spectrum, see Figure 3b) spectra are also depicted. A decay is observed for the absorption maximum at 630 nm, attributed to LE. A growing-in occurs for the maxima at 320 and 438 nm, which are assigned to the ICT state. (c) A global analysis of the band integrals BI(310,350), BI(410,460), and BI(600,680) results in a decay time τ_2 of 1.83 ps, with a growing-in (negative A_2, eq 10) for BI(310,350) and BI(410,460), in the spectral range of the ICT absorption. See the caption of Figure 13.

34DCDMA in MeCN (0.2-100 ps).

Figure S8. 34DCDMA in MeCN at 361 nm excitation (305-683 nm). (a) Transient absorption spectra and (b) excited state absorption (ESA) spectra, at pump-probe delay times between 0.2 and 100 ps, after subtraction of the bleach (BL) spectrum and stimulated emission from LE and ICT (SE(LE) and SE(ICT)). The BL and SE (for fluorescence spectrum, see Figure 3c) spectra are also depicted. A decay is observed for the absorption maximum at 330 and 635 nm, attributed to LE. A growing-in occurs around 400 nm, which is assigned to the ICT state. (c) A global analysis of the band integrals BI(315,350), BI(380,430), and BI(610,680) results in a decay time τ_2 of 4.0 ps, with a growing-in (negative A_2, eq 10) for BI(380,430), in the spectral range of the ICT absorption. See the caption of Figure 13.